model parameters to obtain the corresponding single frequency sensitivity kernels:

$$\begin{cases} K^{(v_h)}(\mathbf{x}_r;\mathbf{x}_s;\mathbf{x};\omega) &= \frac{2\omega^2}{v_0^3} u_0(\mathbf{x};\mathbf{x}_s;\omega) G_0(\mathbf{x};\mathbf{x}_r;\omega); \\ K^{(\varepsilon)}(\mathbf{x}_r;\mathbf{x}_s;\mathbf{x};\omega) &= (u_0(\mathbf{x};\mathbf{x}_s;\omega)\partial_{zz} G_0(\mathbf{x};\mathbf{x}_r;\omega) + \partial_{zz} u_0(\mathbf{x};\mathbf{x}_s;\omega) G_0(\mathbf{x};\mathbf{x}_r;\omega)); \\ K^{(\eta)}(\mathbf{x}_r;\mathbf{x}_s;\mathbf{x};\omega) &= \frac{v_0^2}{\omega^2}(\partial_{xx} u_0(\mathbf{x};\mathbf{x}_s;\omega)\partial_{zz} G_0(\mathbf{x};\mathbf{x}_r;\omega) + \partial_{zz} u_0(\mathbf{x};\mathbf{x}_s;\omega)\partial_{xx} G_0(\mathbf{x};\mathbf{x}_r;\omega)); \end{cases} \tag{3}$$

where $u_0(\mathbf{x};\mathbf{x}_s;\omega)$ and $G_0(\mathbf{x};\mathbf{x}_r;\omega)$ are the source wavefield and the receiver Green's function, respectively.

Update direction using the sensitivity kernels

Preconditioned Conjugate Gradient (PCG) method is used to update the model. The preconditioner is the diagonal of the approximate Hessian and the update direction is given as:

$$\mathbf{p}_2 = \frac{1}{\mathrm{diag}(\mathbf{H_a})}\mathbf{p}_1 \tag{4}$$

The approximate Hessian matrix $\mathbf{H_a}$ is given by the product of the Fréchet derivatives matrix and its conjugate transpose: $\mathbf{H_a} = \mathbf{K}^T\mathbf{K}$. The step size is estimated for each parameter using a second order approximation of the objective function $E_1(\alpha) = E(\mathbf{m} + \alpha^T\mathbf{p}_2)$. For a VTI medium, the vector $\mathbf{m}$ is composed of three vectors corresponding to: v_h, ε and η. The vector $\mathbf{p}_2$ is the update vector. Finally, α is the step size vector given as: $\alpha = \begin{bmatrix} \alpha_{v_h} & \alpha_\varepsilon & \alpha_\eta \end{bmatrix}^T$. The step size vector elements are obtained by solving the 3 3 system:

$$\begin{bmatrix} \mathbf{p}_{2_{v_h}}^T(\mathbf{K}_{v_h}^T\mathbf{K}_{v_h})\mathbf{p}_{2_{v_h}} & \mathbf{p}_{2_{v_h}}^T(\mathbf{K}_{v_h}^T\mathbf{K}_{\varepsilon})\mathbf{p}_{2_\varepsilon} & \mathbf{p}_{2_{v_h}}^T(\mathbf{K}_{v_h}^T\mathbf{K}_{\eta})\mathbf{p}_{2_\eta} \\ \mathbf{p}_{2_\varepsilon}^T(\mathbf{K}_{\varepsilon}^T\mathbf{K}_{v_h})\mathbf{p}_{2_{v_h}} & \mathbf{p}_{2_\varepsilon}^T(\mathbf{K}_{\varepsilon}^T\mathbf{K}_{\varepsilon})\mathbf{p}_{2_\varepsilon} & \mathbf{p}_{2_\varepsilon}^T(\mathbf{K}_{\varepsilon}^T\mathbf{K}_{\eta})\mathbf{p}_{2_\eta} \\ \mathbf{p}_{2_\eta}^T(\mathbf{K}_{\eta}^T\mathbf{K}_{v_h})\mathbf{p}_{2_{v_h}} & \mathbf{p}_{2_\eta}^T(\mathbf{K}_{\eta}^T\mathbf{K}_{\varepsilon})\mathbf{p}_{2_\varepsilon} & \mathbf{p}_{2_\eta}^T(\mathbf{K}_{\eta}^T\mathbf{K}_{\eta})\mathbf{p}_{2_\eta} \end{bmatrix} \begin{bmatrix} \alpha_{v_h} \\ \alpha_\varepsilon \\ \alpha_\eta \end{bmatrix} = \begin{bmatrix} \mathbf{p}_{1_{v_h}}^T\mathbf{p}_{2_{v_h}} \\ \mathbf{p}_{1_\varepsilon}^T\mathbf{p}_{2_\varepsilon} \\ \mathbf{p}_{1_\eta}^T\mathbf{p}_{2_\eta} \end{bmatrix} \tag{5}$$

The resulting 3 step sizes take into account a perturbation in the three parameters. Therefore, the trade-off is considered using this approach. For the adjoint state based FWI, the elements of the matrix in the left hand side require additional modeling steps (needed to approximate the matrix elements by finite difference). For the scattering integral (SI) approach only vector-matrix multiplications are required. As a result, no additional modeling is required and the main computation occurs during the construction of the sensitivity matrix and its decomposition. The computation is minor in the following inversion process.

Numerical results

In Figure 1, the first row shows the VTI Marmousi II model. The original Marmousi II velocity model and the density are used to derive ε and δ Thomsen parameters. Then, those parameters are used to compute the horizontal velocity v_h, ε and η parameters. The initial model, shown in the second row of Figure 1, is obtained by considering a zero δ. Actually, long-wavelength δ information is usually obtained from well information and can not be constrained using surface seismic records. Then, we smooth the vertical velocity and ε using a triangular smoother with a 1500 m radius. The resulting models are comparable to the models used by Alkhalifah and Guitton (2016), where v_h and v_{nmo} are smoothed instead. The modeling is performed in the frequency domain using an acoustic VTI Helmholtz solver. We consider a multi-scale inversion approach where 4 frequency bands are considered. Table 1 shows the inversion parameters for each frequency band.

Frequency Band	f_{min} (Hz)	f_{max} (Hz)	Df (Hz)	Number of iterations
1	2.0	4.0	0.25	40
2	3.5	6.0	0.5	40
3	5.5	9.0	0.5	40
4	8.5	12.0	0.5	40

Table 1 *Inversion parameters.*

As the sensitivity of the recorded data to η is minor (Alkhalifah, 2016), it is not updated during the inversion and we keep it fixed as the initial value. We perform a simultaneous inversion of both v_h

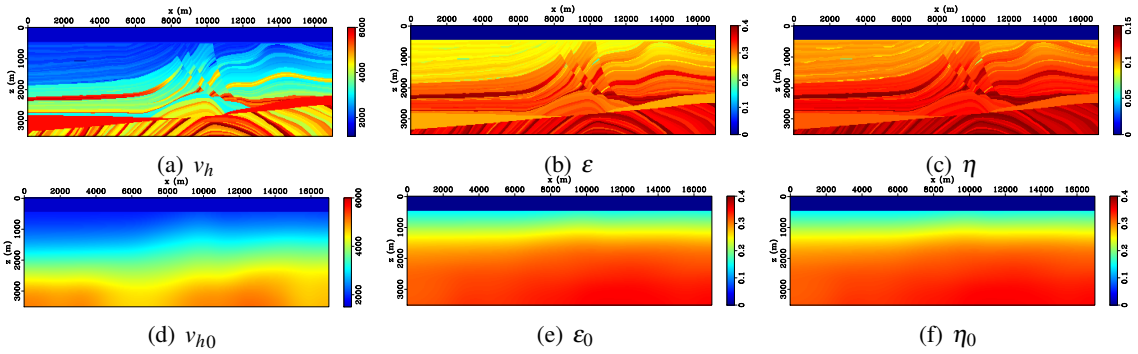

(a) v_h (b) ε (c) η

(d) v_{h0} (e) ε_0 (f) η_0

Figure 1 *Marmousi II VTI model: (a-c) The exact model, (d-f) the initial model.*

and ε parameter. v_h is the main parameter that we aim to invert for and ε plays the secondary role of fitting the amplitude. ε absorbs the inaccuracies in the inversion of short wavelength due to the acoustic approximation. Figure 2 and 3 show the inverted model as well as slices at 7 and 12 km. The horizontal velocity is well inverted and the main features are recovered. We conclude that the acoustic frequency domain multi-parameter inversion using a parameterization based on v_h, ε and η can provide highly resolved and accurate horizontal velocity.

Furthermore, the inverted ε parameter is reasonable and the short wavelength features are well recovered for parts of the model deeper than 1500 m. In fact, the ε parameter is only sensitive to small scattering angles, which results in short wavelength update. From the ε slices, we observe that the shallow part of the initial ε model is far from the true model. Such a difference is not recoverable from the short wavelength update. For the deeper parts, the initial ε is closer to the exact model. As a result, the short wavelength ε update recovers the bumps in the model as seen by Figure 3(c-d). To recover a good ε model, the long wavelength features must exist in the initial model. Also, high frequency information should be used to invert for more accurate short wavelength features. Figure 4 shows the data misfit history for the 4 frequency bands. The misfit is the time domain data over the whole spectrum. The misfit is largely reduced, which shows the convergence of the inversion.

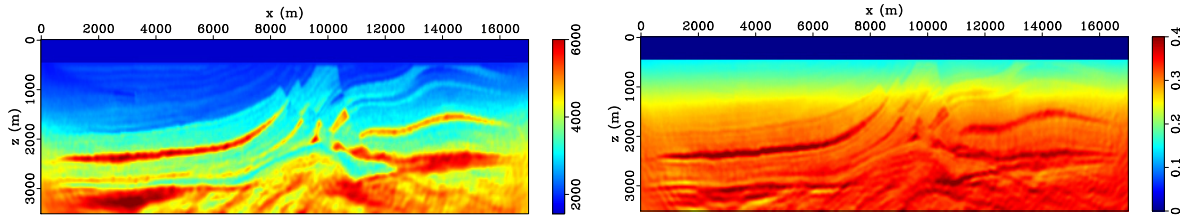

(a) (b)

Figure 2 *Inverted Marmousi II model: (a) v_h and (b) ε.*

Conclusions

We applied a frequency domain FWI using the scattering integral approach to invert VTI medium. The VTI wave equation is parameterized using the horizontal velocity v_h, ε and η anisotropy parameters for reduced trade-off between different parameters. We used a preconditioned conjugate gradient method to update the model. The step size is estimated through a second order approximation of the objective function. It takes into account a perturbation in the three parameters and can take care of the trade-off with no extra modeling cost. The η parameter is kept fixed during the inversion and only v_h and ε are updated. We showed that the method results in accurate inverted models. Finally, we confirmed that the parameterization is suitable for surface recorded seismic data.

Acknowledgements

We would like to thank King Abdullah University of Science and Technology for the financial support. We thank Nabil Masmoudi, Yunseok Choi and all SWAG members for the useful discussions.

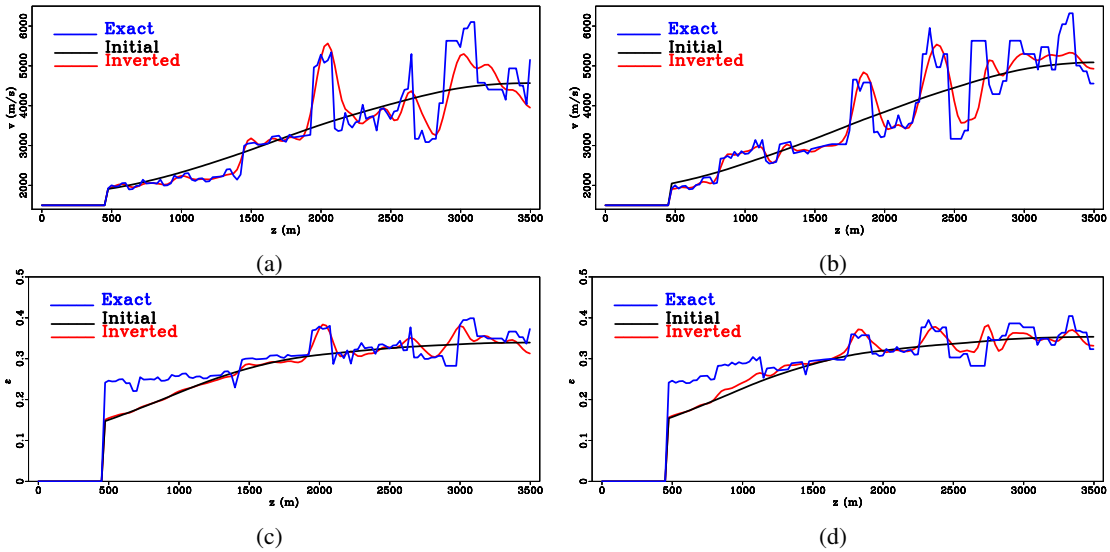

Figure 3 *Inverted Marmousi II model slices: (a,b) v_h slices at 7 and 12 km, (c,d) ε parameter slices at 7 and 12 km.*

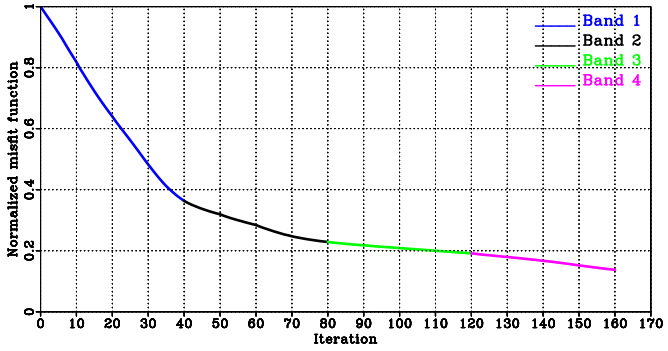

Figure 4 *Data misfit history.*

References

Alkhalifah, T. [2016] Research Note: Insights into the data dependency on anisotropy: an inversion prospective. *Geophysical Prospecting*, **64**(2), 505–513.

Alkhalifah, T. and Guitton, A. [2016] An Optimal Parameterization for Full Waveform Inversion in Anisotropic Media. In: *78th EAGE Conference and Exhibition 2016*.

Alkhalifah, T. and Plessix, R.É. [2014] A recipe for practical full-waveform inversion in anisotropic media: An analytical parameter resolution study. *Geophysics*, **79**(3), R91–R101.

Djebbi, R., Plessix, R.É. and Alkhalifah, T. [2016] Analysis of the traveltime sensitivity kernels for an acoustic transversely isotropic medium with a vertical axis of symmetry. *Geophysical Prospecting*.

Gholami, Y., Brossier, R., Operto, S., Ribodetti, A. and Virieux, J. [2013] Which parameterization is suitable for acoustic vertical transverse isotropic full waveform inversion? Part I: Sensitivity and trade-off analysis. *Geophysics*, **78**(2), R81–R105.

Liu, Y., Yang, J., Chi, B. and Dong, L. [2015] An improved scattering-integral approach for frequency-domain full waveform inversion. *Geophysical Journal International*, **202**(3), 1827–1842.

Plessix, R.É. and Cao, Q. [2011] A parametrization study for surface seismic full waveform inversion in an acoustic vertical transversely isotropic medium. *Geophysical Journal International*, **185**(1), 539–556.

Vigh, D., Cheng, X., Jiao, K., Sun, D. and Kapoor, J. [2014] Multiparameter Full Waveform Inversion on Long-offset Broadband Acquisition-A Case Study. In: *76th EAGE Conference and Exhibition 2014*.

Wu, Z. and Alkhalifah, T. [2016] Waveform inversion for acoustic VTI media in frequency domain. In: *SEG Technical Program Expanded Abstracts 2016*, Society of Exploration Geophysicists, 1184–1189.